Solution processed transition metal oxide anode buffer layers for efficiency and stability enhancement of polymer solar cells

M. Yoosuf Ameen, P. Shamjid, T. Abhijith, V.S. Reddy[*]

Organic and Nano Electronics Laboratory, Department of Physics, National Institute of Technology, Calicut 673601, Kerala, India

A B S T R A C T

Polymer solar cells were fabricated with solution-processed transition metal oxides, MoO_3 and V_2O_5 as anode buffer layers (ABLs). The optimized device with V_2O_5 ABL exhibited considerably higher power conversion efficiency (PCE) compared to the devices based on MoO_3 and poly(3,4-ethylenedioxythiophene):poly(styrene sulfonate) (PEDOT:PSS) ABLs. The space charge limited current measurements and impedance spectroscopy results of hole-only devices revealed that V_2O_5 provided a very low charge transfer resistance and high hole mobility, facilitating efficient hole transfer from the active layer to the ITO anode. More importantly, incorporation of V_2O_5 as ABL resulted in substantial improvement in device stability compared to MoO_3 and PEDOT:PSS based devices. Unencapsulated PEDOT:PSS-based devices stored at a relative humidity of 45% have shown complete failure within 96 h. Whereas, MoO_3 and V_2O_5 based devices stored in similar conditions retained 22% and 80% of their initial PCEs after 96 h. Significantly higher stability of the V_2O_5-based device is ascribed to the reduction in degradation of the anode/active layer interface, as evident from the electrical measurements.

1. Introduction

Interface engineering has gained considerable attention in the field of organic photovoltaics as a means of improving device efficiency and stability. The quality of interfaces between the photoactive layer and the electrodes is very crucial in determining device performance. In a typical polymer solar cell, a buffer layer is inserted between the indium tin oxide (ITO) anode and the active layer for ITO surface smoothening and work function matching [1,2]. This anode buffer layer (ABL) aids in forming an Ohmic contact, which facilitates effective transfer and collection of holes at the anode. Poly(3,4-ethylenedioxythiophene):poly(styrene sulfonate) (PEDOT:PSS) is the most widely used ABL [3–7] owing to its high transparency, high conductivity, and solution processability. However, hygroscopic nature [8–12] of PEDOT:PSS and the instability towards UV-illumination [13,14] lead to fast device degradation. Its acidic nature can corrode ITO anode causing interface instability [15]. As an alternative to PEDOT:PSS, transition metal oxides (TMOs) such as MoO_3, V_2O_5, WO_3, AgO_x, RuO_2, ReO_3, CuO_x, and NiO have been explored as ABLs in polymer solar cells [16–22].

Among different TMOs, MoO_3 and V_2O_5 have gained wide acceptance because of their promising properties like high transparency [23–27], high hole mobility [26,28,29] and a work function [30–33] which matches well with the HOMO level of common donor materials used in polymer solar cells. In contrast to the hygroscopic nature of PEDOT:PSS, MoO_3, and V_2O_5 are more hydrophobic, which enhances adhesion to the active layer and improves environmental stability of the devices [24,33–36]. In spite of the superior properties of MoO_3 and V_2O_5 anode buffer layers, a detailed investigation and an in-depth comparison between them, in terms of device stability and efficiency are still lacking.

Traditionally, thermal evaporation [37,38], atomic layer deposition [39] and sputtering [40,41] were employed for the deposition of TMOs on electrodes. In recent years many researchers have reported different solution processable methods for depositing MoO_3 and V_2O_5 thin films, which are well suited for the fabrication of flexible, large-area and inexpensive organic solar cells. Most of the solution processed methods reported for MoO_3 thin film preparation require either high-temperature annealing [31,42,43] or oxygen plasma treatment [1,44]. Only a very few solution processed methods have been reported on the preparation of V_2O_5 thin films [26,27,29,36]. In the present investigation, we have used the method reported by Murase et al. [23] for MoO_3 thin film preparation and the method reported by Zilberberg et al. [27] for the

* Corresponding author.
  E-mail address: sivaji@nitc.ac.in (V.S. Reddy).

preparation of V_2O_5 thin films, which seem to be very simple and effective and do not require high-temperature annealing or oxygen plasma treatment. Our investigation revealed that the solar cell with V_2O_5 ABL outperforms devices with MoO_3 and PEDOT:PSS ABLs in both efficiency and stability.

2. Experimental

Polymer solar cells with conventional configuration ITO/ABL/P3HT:PCBM/LiF/Al (Fig. 1) have been fabricated with solution processed MoO_3, V_2O_5 and PEDOT:PSS ABLs. The precursor solution of MoO_3 was prepared by heating 0.4 g of ammonium molybdate tetrahydrate [AHM, $(NH4)_6Mo_7O_{24}\cdot4H_2O$] in 10 mL of distilled water at 80 °C for 1 h in air. The MoO_3 solution of desired concentration was obtained by diluting with distilled water. The V_2O_5 solution of required concentration was made by adding the appropriate amount of vanadium(V) oxitriisopropoxide to isopropanol. The patterned ITO substrates with a sheet resistance of 8−12 Ω/sq were cleaned by ultrasonication in detergent, deionized water, methanol, isopropanol, and acetone in sequence, followed by oxygen plasma treatment for 10 min. MoO_3 and V_2O_5 solutions of different concentrations were spin coated on ITO substrates at 4000 rpm for 35 s and then annealed in air at 100 °C for 10 min. For PEDOT:PSS-based devices, PEDOT:PSS was spin-cast on ITO at 5000 rpm for 35 s from 2.8 wt% aqueous solution and annealed at 160 °C for 15 min in the air. The polymer:fullerene active layer blend solution containing 20 mg of poly (3-hexylthiophene) (P3HT) and 20 mg [6,6]-phenyl C_{61} butyric acid methyl ester (PCBM) in 1 mL of 1,2-dichlorobenzene solution was spin coated on the ABL layer at 1000 rpm for 60 s. The active layer was allowed for slow drying for 30 min prior to annealing at 130 °C for 10 min. An LiF layer of 1 nm and an aluminum electrode of 100 nm were thermally evaporated in sequence at a base pressure of 1×10^{-6} mbar. All the devices were having an active area of 9 mm^2. Hole-only devices with structure ITO/ABL/P3HT:PCBM/MoO_3(10 nm)/Al [45−49] were fabricated in the same way as presented above except for the LiF layer, which was replaced with a 10 nm thick thermally evaporated MoO_3 layer. All the materials and reagents were obtained from Sigma-Aldrich and used as received.

The current density-voltage (J-V) measurements were carried out with an Agilent B2902A Source/Measure unit by keeping the devices under AM 1.5 illumination (Photo Emission Tech SS50AAA solar simulator) with a power density of 100 mW/cm^2. The transmission spectra of different ABLs were measured using a UV−vis spectrophotometer (Perkin-Elmer lambda-35). The hole extraction capability of the interfacial layers was investigated using photoluminescence (PL) spectroscopy (Perkin Elmer LS 55 luminescence

spectrophotometer) and impedance spectroscopy (CHI 760E electrochemical workstation). The impedance measurements were performed with an oscillating voltage of 10 mV and frequency of 1 Hz to 1 MHz. Reflection spectroscopy measurement was performed using Shimadzu 2450 spectrophotometer. The chemical composition of precursor solutions of MoO_3 and V_2O_5 was examined using Fourier transform infrared (FT-IR) spectroscopy (Perkin Elmer-Spectrum Two) in attenuated total reflectance (ATR) mode.

3. Results and discussion

Fig. 2a shows the FT-IR spectrum of the MoO_3 precursor solution. The broad absorption band in the range 2600−3600 cm^{-1} is associated with the stretching vibrations of O−H bonds in water molecules. Peak at 1650 cm^{-1} is assigned to the bending vibration of O−H bonds of water and that at 1450 cm^{-1} is assigned to the bending vibration of NH4$^+$ group. The band at 1070 cm^{-1} corresponds to the stretching vibration of Mo−O bonds and the band around 890 cm^{-1} corresponds to the stretching vibration of oxygen in Mo−O−Mo bonds [50]. FT-IR spectrum of V_2O_5 precursor solution is shown in Fig. 2b. The peaks at 3384 and 1624 cm^{-1} are due to stretching and bending vibrational modes of O−H bonds, respectively. The characteristic peaks of V_2O_5 were observed at 991, 770 and 554 cm^{-1}. The peak at 991 cm^{-1} corresponds to the terminal oxygen symmetric stretching mode of V=O and the peaks at 770 and 554 cm^{-1} are associated with the asymmetric and symmetric stretching modes of V−O−V, respectively [51,52]. These spectra confirm the formation of MoO_3 and V_2O_5.

Fig. 3a shows the J-V characteristics of devices with MoO_3 anode buffer layer spin coated from solutions of different MoO_3 concentrations under AM 1.5 illumination. The J-V characteristic of the device without ABL is also included for comparison. Table 1 lists the photovoltaic parameters averaged over 9 devices. The device without ABL shows a very poor performance with a short-circuit current density (J_{sc}) of 4.9 mA/cm^2, an open-circuit voltage (V_{oc}) of 0.58 V, a fill factor (FF) of 44.64%, and a power conversion efficiency (PCE) of 1.27%. Considerable improvement in device performance was noticed with the introduction of MoO_3 ABL. The device with 0.1 wt% MoO_3 solution shows a J_{sc} of 7.31 mA/cm^2, a V_{oc} of 0.59 V, and a FF of 45.39% leading to a PCE of 1.99%. The best average PCE of 2.05% was achieved for the device with 0.5 wt% MoO_3 solution, with a J_{sc} of 7.32 mA/cm^2, a V_{oc} of 0.59 V, and a FF of 47%. With further increase in MoO_3 solution concentration, the device performance deteriorated. It is clear from Table 1 that the increase in film thickness above the optimum value leads to increase in series resistance (R_s) and decrease in shunt resistance (R_{sh}), which lowered the J_{sc} and FF values. As shown in Fig. 3b there is a slight decrease in the transmittance of the MoO_3 film in the wavelength range of 350−650 nm with the increase in MoO_3 solution concentration, leading to a small drop in the amount of light falling on the active layer. This reduces the charge carrier generation in the active layer, contributing to the J_{sc} loss. In the case of devices with MoO_3 ABL, the main source of efficiency loss with an increase in MoO_3 thickness is the lowering of J_{sc} and FF originated from the increase in R_s and decrease in R_{sh}. A similar dependence of device parameters such as J_{sc}, FF, R_s and R_{sh} on the thickness of copper oxide (CuO_x) ABL was also reported [53]. Stubhan et al. improved the efficiency of polymer solar cells using solution processed tungsten trioxide (WO_3) as the ABL [54]. The J_{sc} was insensitive to ABL thickness and the enhancement in efficiency was mainly attributed to increase in FF.

Fig. 4a shows the J-V characteristics of devices with V_2O_5 interlayer spin coated from solutions of different concentrations. Photovoltaic parameters averaged over 9 devices are tabulated in Table 2. The highest average efficiency of 2.65% was achieved for
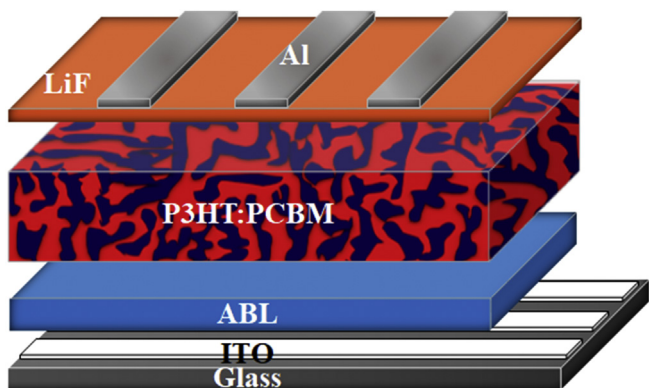

Fig. 1. Architecture of bulk heterojunction polymer solar cell.